Simultaneous single shot rotation-vibration non-equilibrium thermometry using pure rotational fs/ps CARS coherence beating

TIMOTHY Y. CHEN[1,4], NING LIU[1], CHRISTOPHER J. KLIEWER[2], ARTHUR DOGARIU[1], EGEMEN KOLEMEN[1,3], AND YIGUANG JU[1*]

[1] Department of Mechanical and Aerospace Engineering, Princeton University, Princeton, NJ 08544
[2] Sandia National Laboratories, Livermore, CA, 94550
[3] Princeton Plasma Physics Laboratory, Princeton, NJ, 08540
[4] Presently at Sandia National Laboratories, Livermore, CA, 94550
[*] Corresponding author: yju@princeton.edu

Compiled September 22, 2022

We report the development of a simple and sensitive two beam hybrid femtosecond/picosecond pure rotational coherent anti-Stokes Raman scattering (fs/ps CARS) method to simultaneously measure the rotational and vibrational temperatures of diatomic molecules. Rotation-vibration non-equilibrium plays a key role in the chemistry and thermalization in low-temperature plasmas as well as thermal loading of hypersonic vehicles. This approach uses time-domain interferences between ground state and vibrationally excited N_2 molecules to intentionally induce coherence beating that leads to apparent non-Boltzmann distributions in the pure rotational spectra. These distortions enable simultaneous inference of both the rotational and vibrational temperatures. Coherence beating effects were observed in single shot fs/ps CARS measurements of a 75 Torr N_2 DC glow discharge and were successfully modeled for rotational and vibrational temperature extraction. We show that this method can be more sensitive than a pure rotational fs/ps CARS approach using a spectrally narrow probe pulse. Lastly, we experimentally measured the beat frequencies via Fourier transform of the time-domain response and obtained excellent agreement with the model.

http://dx.doi.org/10.1364/ao.XX.XXXXXX

Rotation-vibration (R-V) non-equilibrium measurements are critical for understanding energy transfer and thermalization in low-temperature plasmas and hypersonic vehicles. In plasmas, energy transfer to molecules via collisions with electrons can induce significant vibrational non-equilibrium. Vibrationally-excited molecules are hypothesized to enhance chemical reactivity in plasma-catalysis [1], plasma-assisted combustion [2], and plasma CO2 dissociation [3]. Furthermore, in hypersonic flows, shock-boundary layer interactions can induce R-V non-equilibrium which affects the thermal loading and aerodynamics of hypersonic vehicles [4, 5]. Simultaneous measurements of both the rotational and vibrational temperatures are necessary to further our understanding in these areas.

Hybrid femtosecond/picosecond coherent anti-Stokes Raman scattering (fs/ps CARS) is a powerful laser diagnostic capable of probing gas temperature and species concentrations on the picosecond time scale with tens of microns of spatial resolution [6–17]. A method for retrieving vibrational and rotational temperatures simultaneously from spatially-resolved 1-D rotational fs/ps CARS images was recently developed [11]. This method uses the red-shift of rotational energy levels of vibrationally-excited molecules to measure the vibrational temperature along with the rotational temperature. The key advantages of this approach were the two-beam configuration for straightforward 1-D imaging and the elimination of the need for a separate Stokes pulse generated from an optical parametric amplifier (OPA). However, in [11] a 20 Hz repetition rate picosecond laser with a narrow line-width (~ 0.23 cm^{-1}) was used to resolve the one-sided broadening induced by vibrationally-excited N_2. It would be desirable generate the probe pulse from the femtosecond laser and enable kHz data acquisition rates without a separate laser.

Narrow probe picosecond pulses for fs/ps CARS have been previously generated from femtosecond pulses using second harmonic bandwidth compression (SHBC) [10, 16, 18, 19]. However, these probe pulses typically have 3 to 6 cm^{-1} bandwidths, while the energy spacing between adjacent vibrational levels in the pure rotational spectrum is approximately 1 cm^{-1} in N_2. Therefore, multiple Raman transitions from different vibrational levels will be coherently sampled within the probe pulse bandwidth and they can interfere with one another. This induces so-called "coherence beating" between these Raman transitions and distort the CARS spectrum as a function of probe delay. For example, in the rotational O_2 spectrum, coherence beating occurs due to the electronic triplet configuration of ground state O_2 which splits each rotational energy level into three closely spaced energy levels [20]. For certain probe delays, significant distortion of the CARS spectrum was observed, and accurate temperature

evaluations were not possible without considering the electronic triplet state splitting. In time-resolved CARS, frequency-domain spectra and Raman transition spacings have been obtained by taking the Fourier transform of beat patterns observed in probe delay scans on femtosecond to picosecond time scales [21, 22]. To mitigate coherence beating effects, dual-pump fs/ps CARS was used for R-V non-equilibrium measurements in [10, 23] and recently, simultaneous R-V non-equilibrium measurements were performed using fs/ps CARS in Mach 18 flows [17]. However, such measurements require multiple cameras and an optical parametric amplifier (OPA) to access the vibrational CARS spectrum. This adds complexity and reduces the pulse energy available for generating a CARS signal due to losses in the OPA. It would be desirable to use two-beam fs/ps CARS for R-V non-equilibrium measurements like in [11].

In this Letter, we present a new diagnostic method which instead exploits coherence beating to simultaneously infer the rotational and vibrational temperature from single shot pure rotational fs/ps CARS spectra. We simultaneously retain two-beam fs/ps CARS operation like in [11] and the potential for kHz data acquisition rates like in [15–17]. Furthermore, this approach is applicable to most diatomic molecules. We compare this approach to the frequency-domain one-sided broadening approach previously developed in [11] and show that the coherence beating can be even more sensitive than the one-sided broadening method. A 75 Torr N_2 DC glow discharge was used as a testbed for experimentally demonstrating this technique and vibrational temperatures ranging from 1000 K to 3600 K were measured on a single shot basis.

The detailed theory and principles behind hybrid fs/ps CARS frequency and time-domain modelling can be found in [9–12] and only a brief overview will be given here. Hybrid fs/ps CARS takes advantage of the broadband nature of femtosecond laser pulses to probe multiple Raman transitions simultaneously, while the non-resonant background is avoided with a time delayed spectrally-narrow probe pulse. In this study, two-beam phase matching is used where the both the pump and Stokes photons come from a single fs laser source. The fs/ps CARS time-domain model from [11] was used to calculate the spectral library for fitting the experimental spectra. The principle behind detecting vibrational and rotational energy distributions and their characteristic temperatures simultaneously from rotational CARS is given by Eq. 1 and 2:

$$F(v,J) = B_v(J(J+1)) - D_v(J^2(J+1)^2) \quad \textbf{(1)}$$

$$B_v = B_e - \alpha(v+1/2) + \gamma(v+1/2)^2 \quad \textbf{(2)}$$

where F is the rotational energy of an N_2 molecule in a state (v, J) with v and J being, respectively, the vibrational and rotational energy levels, B_v and D_v the vibrational energy level-dependent rotational and centrifugal constants, B_e is the equilibrium rotational constant, and α and γ are R-V coupling constants. From Eq. 1 and 2, the rotational energy levels exhibit a red-shift with increasing vibrational energy primarily due to the decrease in B_v. This vibrationally-induced shift can be on the order of 1 cm^{-1}. For molecules in R-V non-equilibrium, molecules in the excited vibrational states will appear at these shifted wavelengths. Such shifts have been observed before using spontaneous Raman scattering and nanosecond pulse-width CARS [24–26]. The coherence beating induced by interference between the neighboring vibrational levels allows for inference of the vibrational temperature in the pure rotational CARS spectrum [10, 11]. This approach is similar to [27], where an optimal probe delay for vibrational Q-branch thermometry of N_2 was found due to the interferences between neighboring rotational lines.

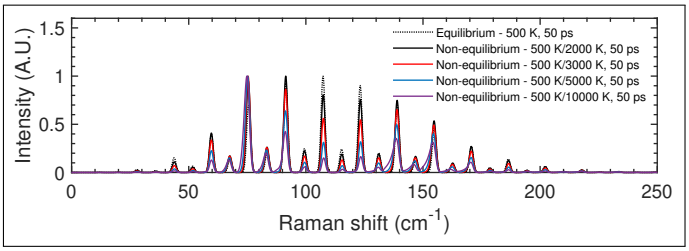

Fig. 1. Comparison of spectra in equilibrium and varying degrees of R-V non-equilibrium at a fixed probe delay of 50 ps.

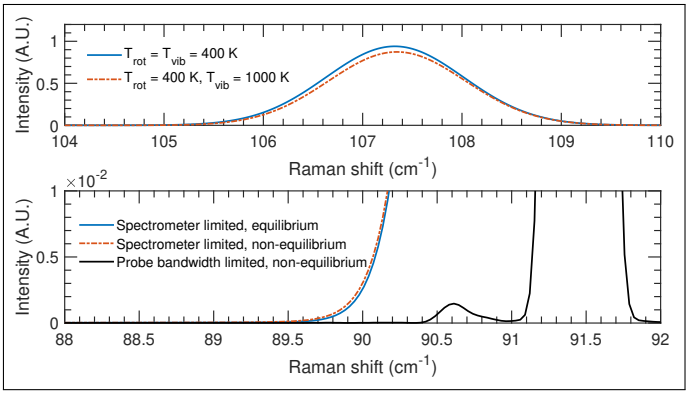

Fig. 2. Sensitivity comparison between coherence beating and one-sided broadening methods for non-equilibrium thermometry at T_{rot} = 400 K and T_{vib} = 1000 K.

Shown in Fig. 1 is a comparison of modelled hybrid fs/ps CARS spectra using a 10 picosecond pulse at an equilibrium temperature of 500 K and non-equilibrium vibrational temperatures up to 10,000 K. A stark difference in both profiles can be seen. The equilibrium spectrum produces an apparent Boltzmann distribution of rotational states. However, the non-equilibrium spectrum is strongly distorted, due to the presence of coherence beating between vibrationally excited N_2 and the ground state N_2. This distortion is a function of the vibrational temperature since the interference will be stronger with larger population of molecules in vibrationally excited states. This can be seen in Fig. 1 where the effects of coherence beating become more severe with higher vibrational temperatures. This suggests that this effect can be leveraged as a sensitive and quantitative diagnostic for simultaneous rotational and vibrational temperature measurements. Furthermore, these intensity distortions are much easier to detect than the one-sided broadening observed in [11]. Therefore, using the time-domain interferences can potentially be more sensitive than when using frequency domain detection. In Fig. 2, we compare the two approaches at a 50 ps delay and a vibrational temperature of 1000 K. If the frequency resolution of the measurement is limited by the probe bandwidth and not the spectrometer, then both techniques can measure this condition. However, typical grating spectrometers have instrument spectral broadening functions of 0.5 to 1 cm^{-1}. In this case, the instrument broadening smears the adjacent peaks and limits the sensitivity of the measurement as shown in the Fig. 2. The equilibrium and non-equilibrium instrument broadened spectra are nearly indistinguishable at this vibrational temperature.

For coherence beating, this is not a problem, and the theoretical sensitivity is retained.

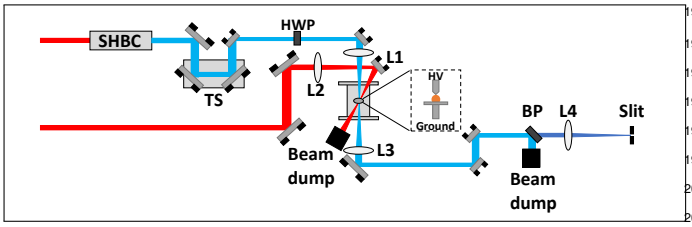

Fig. 3. Experimental fs/ps CARS schematic. L1 to L3: f = 400 mm, L4: f = 75 mm, BP: angle-tuned bandpass filter, TS: translation stage, HWP: half-wave plate.

To experimentally demonstrate this technique, we measured fs/ps CARS spectra on a single shot basis in a 75 Torr N_2 DC glow discharge plasma. Due to the low reduced electric field, efficient pumping of vibrational energy levels induced R-V non-equilibrium in this plasma. However, the DC glow discharge drifted in space, so single shot CARS measurements were necessary since averaging was not possible. The hybrid fs/ps CARS setup is shown in Fig. 3. The 80 fs pump/Stokes pulse centered around 800 nm were supplied by a femtosecond Ti:Sapphire regenerative amplifier (Astrella, Coherent), and a 9 ps probe pulse centered around 399.6 nm was generated using a SHBC design similar to [28]. The probe pulse pulse shape was measured using cross-correlation in pure CH_4 and assumed to be transform-limited (1.63 cm^{-1}). A 1500 gr/mm diffraction grating with 90% diffraction efficiency (Spectrogon) was used as the dispersive element to stretch the femtosecond pulse and the stretched beam was split via a 50/50 beam splitter (Thorlabs). Propagation through the beam splitter and reflection by the beam splitter produces two spatially chirped pulses that are mirror images of each other. In other words, they are oppositely chirped, as required for spectral compression via SHBC. A 250 mm focal length achromatic lens was used to collimate the dispersed light. Since the dispersion was only in one axis, a sheet was formed at the Fourier plane, where the beta barium borate (BBO, Eksma Optics) crystal was placed. Temporal alignment of the split pulses was achieved through adjusting a micrometer translation stage and probe pulses with energies up to 100 μJ were generated. The femtosecond pulse and the picosecond pulse were spherically focused separately and directed to intersect at a 3-degree angle in a two-beam phase matching configuration. The spatial overlap was approximately 1 mm. The time delay between the probe pulse and pump/Stokes pulse was set with a delay line on a motorized translation stage (LTS150, Thorlabs). Detection of the CARS signal was performed via two angle-tuned bandpass filters (Semrock), a Czerny-Turner spectrometer (SP2500i, Princeton Instruments), and an intensified charge coupled device (ICCD, PIMAX1300, Princeton Instruments). The instrument function of the spectrometer was determined via fitting room-temperature N_2 spectra. The plasma reactor was the same as in [11], but the electrodes were swapped for a pin to plane discharge geometry with a pin anode and a 1 cm diameter cylindrical cathode separated by 7 mm. The anode was connected to a high voltage direct current (DC) power supply (Glassman) in series with a 100 kOhm ballast resistor. The voltage at the anode was 500 V and the potential drop across the resistor was 1500 V. The synchronization between the laser and the ICCD was achieved using a delay generator (DG645, Stanford Research Systems) triggered by the femtosecond laser. A constant flow of 600 SCCM of pure N_2 was maintained using a mass flow controller (MKS) and the pressure was kept constant with a downstream automatic throttle valve (153D, MKS).

Shown in Fig. 4 are the experimental spectra of this glow discharge at different probe pulse delays as well as the non-equilibrium fits. The effects of coherence beating on the spectra are immediately obvious from comparison of the data and the R-V equilibrium simulation. Varying the probe delays induced different beat patterns in the rotational spectrum and these coherence beating effects were successfully fit by the CARS model. For the 92 ps delay, a clear deviation from a Boltzmann distribution of rotational states can be seen, while at 44 ps, the distortion is less obvious. This suggests that, like in [27], there should be an optimal probe delay to maximize measurement sensitivity.

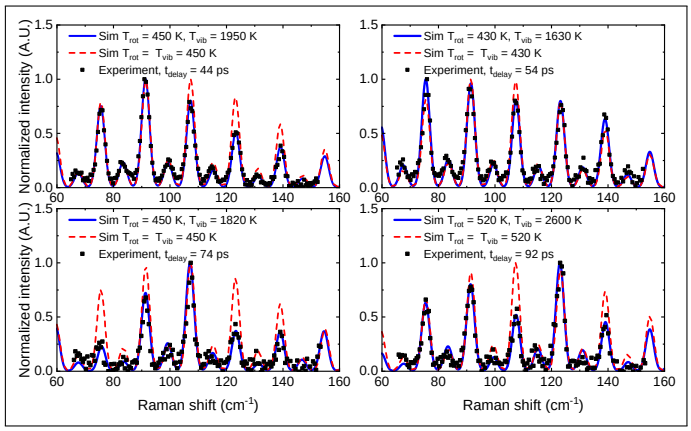

Fig. 4. Single shot fs/ps CARS spectra of a N_2 glow discharge and corresponding simulated fits for R-V non-equilibrium at different probe delays. Equilibrium spectra at the same rotational temperatures were plotted for reference.

The time-dependent R-V non-equilibrium using probe delays of 74 ps and 92 ps were measured in the discharge as shown in Fig. 5. Only spectra with signal to noise ratios above 25 were accepted for temperature evaluation and the 95% confidence intervals of the fits were used as error bars. Both acquisition runs show similar degrees of R-V non-equilibrium and temporal dynamics. The rotational temperature mostly ranged from 350 to 500 K and the vibrational temperature was measured to be within 1000 to 1500 K. However, in both time traces, brief peaks in vibrational temperature up to 3600 K were observed. This likely was due to optimal overlap between the glow discharge and the CARS probe volume.

Lastly, we scanned the probe delay across 300 ps with 10 ps steps to perform time-resolved CARS and used the Fourier transform to retrieve the beat frequencies. Plotted in Fig. 6 are the measured and theoretical beat frequencies. Differences of less than 0.2 cm^{-1} between the theory and experiment was obtained. Considering that the frequency resolution of the Fourier transform was ~0.1 cm^{-1}, this is excellent agreement.

For the present approach, there are several challenges and opportunities for further exploration. Due to the probe bandwidth, individual hot bands remain unresolved, and non-Boltzmann distributions may affect the observed spectra. With the current probe pulse, only vibrational levels up to v=2 are within the probe bandwidth. Therefore, these measurements are primarily sensitive to the first-level vibrational temperature. Additionally,

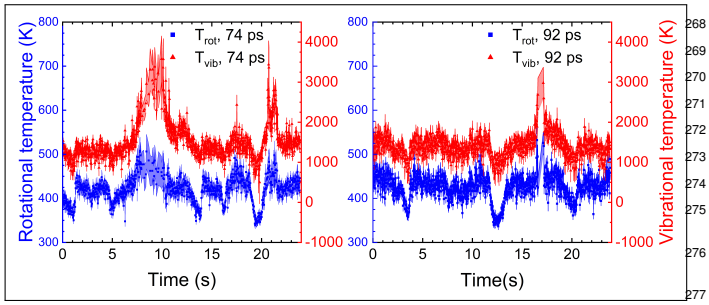

Fig. 5. Time dependent R-V non-equilibrium measured in a N_2 DC glow discharge with probe delays of 74 ps (left) and 92 ps (right). Error bars are shaded.

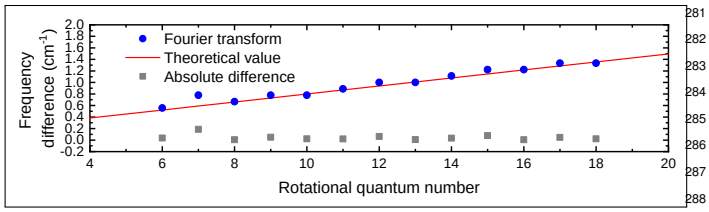

Fig. 6. Measured beat frequencies via Fourier transform of the probe delay scan compared to those calculated by Eq. 1 and 2.

measurements in environments above atmospheric pressure may suffer from signal loss from collisional dephasing prior to the first beat period. Finally, spectral overlap with other molecular species could mask the coherence beating. However, not all lines will overlap, and such effects can be mitigated with a probe delay aligned to the beat periods of spectrally isolated rotational transitions. This may also present an opportunity to simultaneously measure the coherence beating and R-V non-equilibrium of multiple species with an optimized probe delay.

In summary, a new method to simultaneously measure rotational and vibrational temperatures of molecules using coherence beating of pure rotational hybrid fs/ps CARS was developed. The distortion of the pure rotational fs/ps CARS spectrum increased with the vibrational temperature, which indicated that both rotational and vibrational temperature can be directly retrieved from the pure rotational fs/ps CARS spectrum. Coherence beating between rotational lines of vibrationally excited and ground state N_2 was observed experimentally in a N_2 DC glow discharge and the measured beat patterns were in excellent agreement with the model. Furthermore, the extraction of the rotational and vibrational temperatures from fitting the fs/ps CARS spectra distorted by the coherence beating was demonstrated. This technique was shown to be more sensitive than using one-sided broadening like in [11]. Moreover, the switch to measurement of intensity distortions in the spectra enables the possibility of sensitive 2-D R-V non-equilibrium measurements using hyperspectral 2D-CARS [8, 13] as well as high speed kHz two-beam fs/ps CARS of R-V non-equilibrium in plasmas and hypersonic wind tunnels.

Funding. U.S. Department of Energy (DE-FE0026825,DE-NA0003525, DE-SC0020233); National Science Foundation (CBET 1903362).

Acknowledgments. TYC was partially supported by the Program in Plasma Science and Technology Fellowship (PPST). YJ would like to thank the funding support of DOE Plasma Science Center, NETL UCFER, and National Science Foundation grants. TYC, EK, and YJ acknowledge the support of ExxonMobil through its membership in the Princeton E-filliates Partnership of the Andlinger Center for Energy and the Environment. CJK was supported by the Office of Chemical Sciences, Geosciences, and Biosciences, Office of Basic Energy Sciences, U.S. Department of Energy. Sandia National Laboratories is a multi-mission laboratory managed and operated by National Technology and Engineering Solutions of Sandia, LLC, a wholly owned subsidiary of Honeywell International, Inc., for the U.S. Department of Energy's National Nuclear Security Administration.

Disclosures. The authors declare no conflicts of interest.

Data availability. Data underlying the results presented in this paper are not publicly available at this time but may be obtained from the authors upon reasonable request.

REFERENCES

1. P. Mehta, P. Barboun, F. A. Herrera, J. Kim, P. Rumbach, D. B. Go, J. C. Hicks, and W. F. Schneider, Nat. Catal. **1**, 269 (2018).
2. X. Mao, Q. Chen, A. C. Rousso, T. Y. Chen, and Y. Ju, Combust. Flame **206**, 522 (2019).
3. T. Kozák and A. Bogaerts, Plasma Sources Sci. Technol. **23**, 045004 (2014).
4. I. Armenise, M. Capitelli, G. Colonna, and G. Gorse, J. Thermophys. Heat Transf. **10**, 397 (1996).
5. J. D. Reinert, G. V. Candler, and J. R. Komives, AIAA J. **58**, 4055 (2020).
6. B. D. Prince, A. Chakraborty, B. M. Prince, and H. U. Stauffer, The J. Chem. Phys. **125**, 044502 (2006).
7. D. Pestov, R. K. Murawski, G. O. Ariunbold, X. Wang, M. Zhi, A. V. Sokolov, V. A. Sautenkov, Y. V. Rostovtsev, A. Dogariu, Y. Huang, and M. O. Scully, Science **316**, 265 (2007).
8. A. Bohlin and C. J. Kliewer, The J. Chem. Phys. **138**, 221101 (2013).
9. H. U. Stauffer, J. D. Miller, M. N. Slipchenko, T. R. Meyer, B. D. Prince, S. Roy, and J. R. Gord, The J. Chem. Phys. **140**, 024316 (2014).
10. C. E. Dedic, T. R. Meyer, and J. B. Michael, Optica **4**, 563 (2017).
11. T. Y. Chen, B. M. Goldberg, B. D. Patterson, E. Kolemen, Y. Ju, and C. J. Kliewer, Opt. Lett. **45**, 4252 (2020).
12. T. Y. Chen, C. J. Kliewer, B. M. Goldberg, E. Kolemen, and Y. Ju, Combust. Flame **224**, 183 (2021).
13. J. D. Miller, M. N. Slipchenko, J. G. Mance, S. Roy, and J. R. Gord, Opt. Express **24**, 24971 (2016).
14. J. E. Retter, G. S. Elliott, and S. P. Kearney, Combust. Flame **191**, 527 (2018).
15. K. A. Rahman, E. L. Braun, M. N. Slipchenko, S. Roy, and T. R. Meyer, Opt. Lett. **45**, 503 (2020).
16. L. Castellanos, F. Mazza, D. Kliukin, and A. Bohlin, Opt. Lett. **45**, 4662 (2020).
17. A. Dogariu, L. E. Dogariu, M. S. Smith, B. McManamen, J. F. Lafferty, and R. B. Miles, "Velocity and Temperature Measurements in Mach 18 Nitrogen Flow at Tunnel 9," in *AIAA Scitech 2021 Forum,* (2021).
18. F. Raoult, A. C. L. Boscheron, D. Husson, C. Sauteret, A. Modena, V. Malka, F. Dorchies, and A. Migus, Opt. Lett. **23**, 1117 (1998).
19. S. P. Kearney and D. J. Scoglietti, Opt. Lett. **38**, 833 (2013).
20. T. L. Courtney and C. J. Kliewer, The J. Chem. Phys. **149**, 234201 (2018).
21. H. Graener, J. W. Nibler, and A. Laubereau, Opt. Lett. **9**, 165 (1984).
22. A. Dogariu, Y. Huang, Y. Avitzour, R. K. Murawski, and M. O. Scully, Opt. Lett. **31**, 3176 (2006).
23. C. E. Dedic and J. B. Michael, Combust. Flame **227**, 322 (2021).
24. J. J. Barrett and A. B. Harvey, J. Opt. Soc. Am. **65**, 392 (1975).
25. R. E. Teets and J. H. Bechtel, Opt. Lett. **6**, 458 (1981).
26. A. Bohlin, F. Vestin, P. Joubert, J. Bonamy, and P.-E. Bengtsson, J. Raman Spectrosc. **40**, 788 (2009).
27. J. D. Miller, C. E. Dedic, and T. R. Meyer, J. Raman Spectrosc. **46**, 702 (2015).
28. K. E. Thorn, N. R. Monahan, S. K. K. Prasad, K. Chen, and J. M. Hodgkiss, Opt. Express **26**, 28140 (2018).

FULL REFERENCES

1. P. Mehta, P. Barboun, F. A. Herrera, J. Kim, P. Rumbach, D. B. Go, J. C. Hicks, and W. F. Schneider, "Overcoming ammonia synthesis scaling relations with plasma-enabled catalysis," Nat. Catal. **1**, 269–275 (2018).
2. X. Mao, Q. Chen, A. C. Rousso, T. Y. Chen, and Y. Ju, "Effects of controlled non-equilibrium excitation on H2/O2/He ignition using a hybrid repetitive nanosecond and DC discharge," Combust. Flame **206**, 522–535 (2019).
3. T. Kozák and A. Bogaerts, "Splitting of CO_2 by vibrational excitation in non-equilibrium plasmas: a reaction kinetics model," Plasma Sources Sci. Technol. **23**, 045004 (2014).
4. I. Armenise, M. Capitelli, G. Colonna, and G. Gorse, "Nonequilibrium vibrational kinetics in the boundary layer of re-entering bodies," J. Thermophys. Heat Transf. **10**, 397–405 (1996).
5. J. D. Reinert, G. V. Candler, and J. R. Komives, "Simulations of Unsteady Three-Dimensional Hypersonic Double-Wedge Flow Experiments," AIAA J. **58**, 4055–4067 (2020).
6. B. D. Prince, A. Chakraborty, B. M. Prince, and H. U. Stauffer, "Development of simultaneous frequency- and time-resolved coherent anti-Stokes Raman scattering for ultrafast detection of molecular Raman spectra," The J. Chem. Phys. **125**, 044502 (2006).
7. D. Pestov, R. K. Murawski, G. O. Ariunbold, X. Wang, M. Zhi, A. V. Sokolov, V. A. Sautenkov, Y. V. Rostovtsev, A. Dogariu, Y. Huang, and M. O. Scully, "Optimizing the Laser-Pulse Configuration for Coherent Raman Spectroscopy," Science **316**, 265–268 (2007).
8. A. Bohlin and C. J. Kliewer, "Communication: Two-dimensional gas-phase coherent anti-Stokes Raman spectroscopy (2D-CARS): Simultaneous planar imaging and multiplex spectroscopy in a single laser shot," The J. Chem. Phys. **138**, 221101 (2013).
9. H. U. Stauffer, J. D. Miller, M. N. Slipchenko, T. R. Meyer, B. D. Prince, S. Roy, and J. R. Gord, "Time- and frequency-dependent model of time-resolved coherent anti-Stokes Raman scattering (CARS) with a picosecond-duration probe pulse," The J. Chem. Phys. **140**, 024316 (2014).
10. C. E. Dedic, T. R. Meyer, and J. B. Michael, "Single-shot ultrafast coherent anti-Stokes Raman scattering of vibrational/rotational nonequilibrium," Optica **4**, 563 (2017).
11. T. Y. Chen, B. M. Goldberg, B. D. Patterson, E. Kolemen, Y. Ju, and C. J. Kliewer, "1-D imaging of rotation-vibration non-equilibrium from pure rotational ultrafast coherent anti-Stokes Raman scattering," Opt. Lett. **45**, 4252–4255 (2020).
12. T. Y. Chen, C. J. Kliewer, B. M. Goldberg, E. Kolemen, and Y. Ju, "Time-domain modelling and thermometry of the CH_4 ν_1 Q-branch using hybrid femtosecond/picosecond coherent anti-Stokes Raman scattering," Combust. Flame **224**, 183–195 (2021).
13. J. D. Miller, M. N. Slipchenko, J. G. Mance, S. Roy, and J. R. Gord, "1-kHz two-dimensional coherent anti-Stokes Raman scattering (2D-CARS) for gas-phase thermometry," Opt. Express **24**, 24971 (2016).
14. J. E. Retter, G. S. Elliott, and S. P. Kearney, "Dielectric-barrier-discharge plasma-assisted hydrogen diffusion flame. Part 1: Temperature, oxygen, and fuel measurements by one-dimensional fs/ps rotational CARS imaging," Combust. Flame **191**, 527–540 (2018).
15. K. A. Rahman, E. L. Braun, M. N. Slipchenko, S. Roy, and T. R. Meyer, "Flexible chirp-free probe pulse amplification for kHz fs/ps rotational CARS," Opt. Lett. **45**, 503 (2020).
16. L. Castellanos, F. Mazza, D. Kliukin, and A. Bohlin, "Pure-rotational 1D-CARS spatiotemporal thermometry with a single regenerative amplifier system," Opt. Lett. **45**, 4662 (2020).
17. A. Dogariu, L. E. Dogariu, M. S. Smith, B. McManamen, J. F. Lafferty, and R. B. Miles, "Velocity and Temperature Measurements in Mach 18 Nitrogen Flow at Tunnel 9," in *AIAA Scitech 2021 Forum,* (2021).
18. F. Raoult, A. C. L. Boscheron, D. Husson, C. Sauteret, A. Modena, V. Malka, F. Dorchies, and A. Migus, "Efficient generation of narrow-bandwidth picosecond pulses by frequency doubling of femtosecond chirped pulses," Opt. Lett. **23**, 1117–1119 (1998).
19. S. P. Kearney and D. J. Scoglietti, "Hybrid femtosecond/picosecond rotational coherent anti-Stokes Raman scattering at flame temperatures using a second-harmonic bandwidth-compressed probe," Opt. Lett. **38**, 833–835 (2013).
20. T. L. Courtney and C. J. Kliewer, "Rotational coherence beating in molecular oxygen: Coupling between electronic spin and nuclear angular momenta," The J. Chem. Phys. **149**, 234201 (2018).
21. H. Graener, J. W. Nibler, and A. Laubereau, "Picosecond coherent anti-Stokes Raman spectroscopy of molecules in free jet expansions," Opt. Lett. **9**, 165 (1984).
22. A. Dogariu, Y. Huang, Y. Avitzour, R. K. Murawski, and M. O. Scully, "Sensitive femtosecond coherent anti-Stokes Raman spectroscopy discrimination between dipicolinic acid and dinicotinic acid," Opt. Lett. **31**, 3176 (2006).
23. C. E. Dedic and J. B. Michael, "Thermalization dynamics in a pulsed microwave plasma-enhanced laminar flame," Combust. Flame **227**, 322–334 (2021).
24. J. J. Barrett and A. B. Harvey, "Vibrational and rotational–translational temperatures in N_2 by interferometric measurement of the pure rotational Raman effect," J. Opt. Soc. Am. **65**, 392 (1975).
25. R. E. Teets and J. H. Bechtel, "Coherent anti-Stokes Raman spectra of oxygen atoms in flames," Opt. Lett. **6**, 458 (1981).
26. A. Bohlin, F. Vestin, P. Joubert, J. Bonamy, and P.-E. Bengtsson, "Improvement of rotational cars thermometry in fuel-rich hydrocarbon flames by inclusion of n2-h2 raman line widths," J. Raman Spectrosc. **40**, 788–794 (2009).
27. J. D. Miller, C. E. Dedic, and T. R. Meyer, "Vibrational femtosecond/picosecond coherent anti-Stokes Raman scattering with enhanced temperature sensitivity for flame thermometry from 300 to 2400 K: Femtosecond/picosecond coherent anti-Stokes Raman scattering," J. Raman Spectrosc. **46**, 702–707 (2015).
28. K. E. Thorn, N. R. Monahan, S. K. K. Prasad, K. Chen, and J. M. Hodgkiss, "Efficient and tunable spectral compression using frequency-domain nonlinear optics," Opt. Express **26**, 28140 (2018).